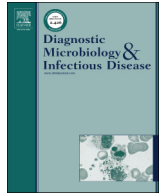




Since January 2020 Elsevier has created a COVID-19 resource centre with free information in English and Mandarin on the novel coronavirus COVID-19. The COVID-19 resource centre is hosted on Elsevier Connect, the company's public news and information website.

Elsevier hereby grants permission to make all its COVID-19-related research that is available on the COVID-19 resource centre - including this research content - immediately available in PubMed Central and other publicly funded repositories, such as the WHO COVID database with rights for unrestricted research re-use and analyses in any form or by any means with acknowledgement of the original source. These permissions are granted for free by Elsevier for as long as the COVID-19 resource centre remains active.



Initial performance evaluation of a spotted array Mobile Analysis Platform (MAP) for the detection of influenza A/B, RSV, and MERS coronavirus ☆☆☆

Justin Hardick ^{a,*}, David Metzgar ^b, Lisa Risen ^b, Christopher Myers ^c, Melinda Balansay ^c, Trent Malcom ^d, Richard Rothman ^d, Charlotte Gaydos ^a

^a Johns Hopkins University School of Medicine, Division of Infectious Diseases, Baltimore, MD, USA

^b Ibis Biosciences, Carlsbad, CA, USA

^c Naval Health Research Center, San Diego, CA, USA

^d Johns Hopkins University Department of Emergency Medicine, Baltimore, MD, USA

ARTICLE INFO

Article history:

Received 6 November 2017

Received in revised form 26 January 2018

Accepted 15 February 2018

Available online 17 February 2018

Keywords:

Respiratory viruses

Point-of-care diagnostics

MERS

ABSTRACT

Clinical samples were evaluated with the Mobile Analysis Platform (MAP) to determine platform performance for detecting respiratory viruses in samples previously characterized using clinical reverse transcriptase polymerase chain reaction assays. The percent agreement between MAP and clinical results was 97% for influenza A (73/75), 100% (21/21) for influenza B, 100% (6/6) for respiratory syncytial virus (RSV), and 80% (4/5) for negative specimens. The approximate limit of detection of the MAP was 30 copies/assay for RSV and 1500 copies/assay for Middle East respiratory syndrome coronavirus.

© 2018 Elsevier Inc. All rights reserved.

Acute respiratory illnesses (ARIs) caused by respiratory viruses including influenza viruses and respiratory syncytial virus (RSV) affect hundreds of millions of people per year and are the most common causes of viral infections in the respiratory tract in humans (Berry et al., 2015; Fendrick et al., 2003; Zimmerman et al., 2015). Each year, approximately 500 million cases of ARI are reported in the United

States, with direct and indirect costs approaching \$40 billion annually (Berry et al., 2015; Fendrick et al., 2003).

The 2009 H1N1 pandemic strain of influenza and the H3N2 seasonal variant that circulated during the 2014–2015 season serve as examples of the importance of continued respiratory virus surveillance efforts, and the importance of using accurate and inclusive diagnostics in respiratory virus management (Flannery et al., 2016; Mahony, 2010; Mahony et al., 2011). In addition, given the emergence of Middle East respiratory syndrome (MERS) coronavirus and subsequent outbreaks thereof in the Middle East and South Korea, it is important that diagnostic assays for respiratory viruses are rapid and deployable at or near the point of care (POC) (Bhadra et al., 2015; Raj et al., 2014). Such diagnostic platforms are becoming more common and are capable of detecting a wide array of respiratory pathogens (Zumla et al., 2014).

We evaluated a novel, portable, near-POC diagnostic platform, the Mobile Analysis Platform (MAP), by assessing the capability of the MAP to detect influenza A, influenza B, and RSV in externally extracted clinical samples, and by establishing the platform's limit of detection (LOD) for RSV and MERS in clinical matrices.

The MAP is a small, portable device integrating disposable assay-specific microfluidic cards (Fig. 1). The MAP system is equipped with a set of subsystem to allow for automatic assay processing. This includes A) a barcode reader to input both specimen and microfluidic card serial numbers; B) a motorized system to crush liquid reagent

☆ Funding Statement: This work was supported in part by the National Institute of Allergy and Infectious Diseases Contract HHSN272201400007C awarded to the Johns Hopkins Center for Influenza Research and Surveillance (JHCEIRS) at the Johns Hopkins University. Any opinions, findings, conclusions, or recommendations expressed in this publication are those of the authors and do not represent the policy or position of the National Institute of Allergy and Infectious Disease or the National Institutes of Health. This research was developed with funding from the Defense Advanced Research Projects Agency (DARPA). The views, opinions, and/or findings expressed are those of the author and should not be interpreted as representing the official views or policies of the Department of the Navy, Department of the Army, Department of the Air Force, Department of Veterans Affairs Department of Defense, or the US Government. Approved for public release; distribution unlimited.

☆☆ Christopher A. Myers is an employee of the US Government and this work was prepared as part of his official duties. Title 17, U.S.C. §105 provides the "Copyright protection under this title is not available for any work of the United States Government". Title 17, U.S.C. §101 defines a US Government work as work prepared by an employee of the US Government as part of that person's official duties.

* Corresponding author. Tel.: +443-287-5403.

E-mail address: jhardic1@jhmi.edu (J. Hardick).

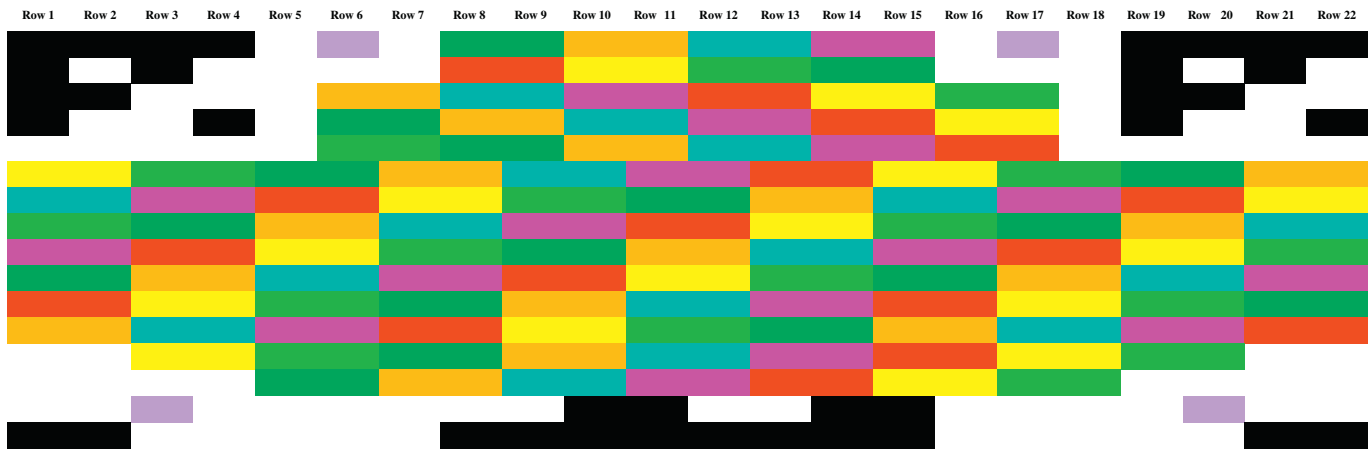


Fig. 1. Respiratory array card design for the MAP unit. 1) Black squares indicate the position of fiducial spots used to home the camera prior to reading the array card. 2) Light purple squares indicate the position of hybridization control spots. 3) Dark green squares indicate MERS target hybridization spots. 4) Dark yellow squares indicate the position of influenza A virus target hybridization spots. 5) Light blue squares indicate the position of influenza B virus target hybridization spots. 6) Dark purple squares indicate the position of RSV target hybridization spots. 7) Red squares indicate the position of array spots that are open and could accommodate other respiratory virus targets. 8) Light yellow squares indicate internal control target hybridization spots. 9) Light green squares indicate human DNA target hybridization spots.

packs on command; C) a pneumatic system (air pressure and vacuum) to move liquids within the cards via peristaltic pumping using vacuum-actuated midstream valves (specimens are thus mixed with various reagents prepackaged into the cards in lyophilized beads to move sample and reagents on the microfluidics card); and D) a set of thermal electric coolers to allow for rapid polymerase chain reaction (PCR; 30 min for 40 cycles) PCR cycling of the mixed sample and reagents is performed in a chamber sandwiched between 2 thermoelectric cooling devices; E) heating elements to maintain temperature at a separate hybridization chamber; F) an optics system that includes a LED for dye excitation and CCD camera for imaging the microarray; G) an ARM processor; H) an LCD screen; and I) keypad.

The microfluidics card is disposable and has all the materials required for the assay including A) sample port to load the swab, B) wet reagents held in sealed blister packs, C) lyophilized reagents, and D) a microarray chip. The microarray chip consists of 100- μm spots of specific DNA capture probes. The array has 400 of these features, with 100 features reserved for image alignment. This allows up to 300 separate spots for the assay. PCR products are then digested using uracil deglycosylase and hybridized to a spotted microarray and washed. The microarray is then imaged with a digital camera and LED illumination, and the image is analyzed and statistically interpreted via onboard analysis software. The entire process is fully automated, and results are presented as positive/negative/invalid declarations on the screen of the MAP unit. Multiple primer pair/probe combinations are employed for each analyte, each of which is designed to offer maximum breadth of coverage within the known diversity of the targeted viral genus.

A total of 130 clinical respiratory virus samples were evaluated, including both nasopharyngeal swab samples resuspended in VTM ($N = 85$) and nasal wash samples ($N = 45$) composed of true positives for influenza A ($N = 93$), influenza B ($N = 21$), and RSV ($N = 7$), and samples that were negative for these analytes ($N = 9$). Samples were acquired through institutional review board-approved studies (IRB00052743, NHRC.2015.0033) from adults ≥ 18 years old that were symptomatic for a respiratory virus infection. Influenza A and B samples previously tested positive via the Cepheid Xpert Flu assay (Cepheid, Sunnyvale, CA) or CDC Human Influenza Virus Real-Time PCR Diagnostic Panel (US Centers for Disease Control and Prevention, Atlanta, GA), while RSV samples previously tested positive via a published real-time PCR assay (Templeton et al., 2004). LOD experiments were performed for RSV and MERS by spiking virus into negative clinical matrix. When available, leftover extracts from initial clinical diagnostic testing were

utilized. When these were not available, the same methods were used to generate new extracts from waste aliquots of the specimens. Nucleic acids were extracted using either the Arrow Viral NA Kit (NorDiag) or the DSP Viral Mini Kit (Qiagen). Extracted nucleic acid was loaded onto individual MAP assay cards, which were then run and analyzed on portable MAP devices according to the manufacturer's instructions. Primer sequences for the target organisms can be found in Table 1, with reagent concentrations for the array cards listed in Table 2.

Cycling conditions were as follows: RT step, 5 min at 52 °C; Hotstart step, 30 s at 95 °C; and extended touchdown PCR and fast PCR, 1 cycle of 7 s at 95 °C, 1 s at 55 °C, 30 s at 69.5 °C, 2 s at 80 °C followed by 1 cycle of 7 s at 95 °C, 1 s at 53.5 °C, 30 s at 67 °C, 2 s at 80 °C followed by 1 cycle of 7 s at 95 °C, 1 s at 51 °C, 30 s at 65 °C, 2 s at 80 °C followed by 1 cycle of 7 s at 95 °C, 1 s at 50 °C, 30 s at 63 °C, 2 s at 80 °C followed by 1 cycle of 7 s at 95 °C, 1 s at 49 °C, 30 s at 62 °C, 2 s at 80 °C followed by 35 cycles of 7 s at 95 °C, 1 s at 45 °C, 5 s at 65 °C and 2 s at 80 °C. All ramp rates on approach to 80 °C were dampened to 20% of maximum. Time to result including nucleic acid extraction was 110 min per sample. All results are reported here as they appeared on the automated output of the MAP devices. Samples that generated either an invalid result or an error report were recorded as assay failures and were not repeated.

Percent agreement between MAP and standard-of-care reverse transcriptase PCR results was 97% (73/75) for influenza A-positive samples, with 2 false-negative results and 18 assay failures resulting in invalid or error reports. Percent agreement for influenza B was 100% (21/21) with no assay failures and 100% (6/6) for RSV with 1 assay failure. Agreement was 80% (4/5) for negative samples, with 1 RSV-positive result and 4 assay failures. The LOD established was 30 and 1500 copies of virus/assay for RSV and MERS coronavirus, respectively.

Previous epidemics and pandemics, as well as the emergence of new respiratory viral pathogens, highlight the need for accurate diagnostic platforms capable of being deployed near the POC (Zumla et al., 2014). We performed an evaluation of the MAP prototype to determine its capability to detect and identify influenza A, influenza B, and RSV, and performed LOD experiments in clinical matrix for RSV and MERS. Percent agreement between the MAP assay result and the predicate result were high for all pathogens evaluated (97–100%) when excluding invalid assay card results and error reports (no-test instances), and LOD experiments for RSV and MERS yielded acceptable LODs.

An ideal evaluation would have included enough positive and negative samples to calculate sensitivity and specificity at the lower bound of the

Table 1
Primer sequences and targets for MAP respiratory virus array.

Organism	Molecular target	Product size (bp ^a)	Primer name	Sequence
Influenza A	M1	110	VIR13095F VIR13096R	TCAGGCUCCUCAAGCCGA /5MAXN ^b /TGCAGGATTGGTCTTGCTTTAICCA
Influenza A	PA	74	VIR13099F VIR13100R	CTUGAGAAUUTUAGAGCCUATGUGAUGG /5MAXN/CACATTTGAGAAAGCTTGGCCTCAAT
Influenza B	PB1	83	VIR13470F VIR13471R	CAGGCAGCAAUTUCAACAACATUCCC /5MAXN/TTGTCTATTGTGTAGCCTGTCTCTGTTC
Influenza B	PA	78	VIR13491F VIR13492R	GGAGGGAAAAUCUGTGUACCTGUATUGC /5MAXN/TAGCTTCCATTCCTCCATTTCAITTTGGAT
RSV	Matrix protein	83	VIR13361F VIR13363R	AAGAUGGGGCAAUAUGGAAACAUCUGGAA /5MAXN/TAGAACATTGTACTGAACAGCTGTGTGA
RSV	Phosphoprotein	84	VIR13362R VIR13355F VIR13357F VIR13356R	/5MAXN/TAGGACATTGTATTGAACAGCAGCTGTGA TCGGCUCGUGAUGGAAUAAGAGAUGC TCUGCUCGGGAUGGUATAAGAGAUGC /5MAXN/CGTCATTAATGCTTCAGTCTGATTTTTCTATCAT
MERS	Orf1A protein	92	VIR13358R VIR13088F VIR13089R	/5MAXN/CGTCATTAATGCTTCGTCTTATTTTTCTATCAT CGGCCUUAACUGGUUGUUGUU /5MAXN/AGCATAATTGTATGACCCGACGTC
MERS	N protein	102	VIR13090F VIR13091R	CCUGUGUACUUCUUCGGUACAGU /5MAXN/GTAGGCATCAATTTTTGCTCAAGAAGC

Organism targets, predicted PCR product size, primer name, and primer sequences are listed here.

^a Base pairs.

^b 5MAX (NHS ester).

95% confidence interval, as opposed to calculating percent agreement. However, based on the limited number of array cards available for this evaluation, it was more important to evaluate as many positive samples as possible to gauge the capability of the array cards to amplify pathogens.

For MERS, an ideal evaluation would have included clinical samples; however, given the rarity and difficulty in acquiring MERS positive clinical samples, this was not possible for this evaluation.

In instances where an invalid result was generated, it was almost exclusively the result of variable fluid handling in the array card,

which could be overcome by modifying the technology utilized for fluid handling on the MAP unit. Additional improvements to the MAP unit would also include combining the extraction and amplification process into one instrument, which would bring the MAP unit closer to being a POC diagnostic and meeting ASSURED criteria.

Clearly, there are limitations to the study; most notably, sensitivity and specificity for the assay were not calculated due to the low number of negative samples evaluated. Future studies would ideally include a large increase in the number of negative samples evaluated, as well as performing the study in a prospective manner.

While this technology is in early stages of development and, as such, yielded a high rate of invalid (no test) results, percent agreement with clinical laboratory methods approached 97% for completed tests. This technology shows promise as a rapid, accurate, deployable diagnostic technology for automated detection and discrimination of multiple pathogens in clinical sample extracts.

Table 2
Reagent concentrations for the MAP respiratory virus assay cards.

<i>UDG (Excipient X4) – 100 µL in digestion well</i>
10 U UDG
3% Trehalose
1.5 mmol/L Tris
7.5 mmol/L KCL
0.015 mmol/L EDTA
0.15 mmol/L DTT
0.0015 % BSA
50.00 nM hybridization control
<i>Kapa (Excipient X2.2) – 150 µL in PCR Master Mix chamber</i>
16 U Kapa
2 % Trehalose
266.67 µmol/L dNTP mixture
4.67 mmol/L MgCL ₂
1.33 X Buffer A
<i>SSIII (Excipient A) – 150 µL in MM chamber^c</i>
50 U SuperScript III
2 % Trehalose
5 mmol/L Tris
1 mmol/L ammonium sulfate
1.2 mmol/L MgCL ₂
0.005 % Tween-40
0.4 mmol/L DTT
0.015 µg random primers
0.03 µg Poly-A

Composition of each of the 3 lyophilized bead reagents provided with the Map cards, and the resulting reagent concentrations or compositions following resuspension thereof in the chambers of the card in which the beads were packaged are represented. Super Script III (Life Technologies, Carlsbad, CA).

References

Berry M, Gamielien J, Fielding BC. Identification of new respiratory viruses in the new millennium. *Virus* 2015:996–1019.

Bhadra S, Jiang YS, Kumar MR, Johnson RF, Hensley LE, Ellington AD. Real-time sequence-validated loop-mediated isothermal amplification assays for detection of Middle East respiratory syndrome coronavirus (MERS-CoV). *PLoS One* 2015:e0123126.

Fendrick AM, Monto AS, Nightengale B, Sarnes M. The economic burden of non-influenza-related viral respiratory tract infection in the United States. *Arch Intern Med* 2003; 487–94.

Flannery B, Zimmerman RK, Gubareva LV, Garten RJ, Chung JR, Nowalk MP, et al. Enhanced genetic characterization of influenza A(H3N2) viruses and vaccine effectiveness by genetic group. 2014–2015. *J Infect Dis* 2016;214:1010–9. [pii: jiw181].

Mahony JB. Nucleic acid amplification-based diagnosis of respiratory virus infections. *Expert Rev Anti Infect Ther* 2010:1273–92.

Mahony JB, Petrich A, Smieja M. Molecular diagnosis of respiratory virus infections. *Crit Rev Clin Lab Sci* 2011:217–49.

Raj VS, Osterhaus AD, Fouchier RA, Haagmans BL. MERS: emergence of a novel human coronavirus. *Curr Opin Virol* 2014:58–62.

Templeton KE, Scheltinga SA, Beersma MF, Kroes AC, Claas EC. Rapid and sensitive method using multiplex real-time PCR for diagnosis of infections by influenza A and influenza B viruses, respiratory syncytial virus, and parainfluenza viruses 1, 2, 3, and 4. *J Clin Microbiol* 2004:1564–9.

Zimmerman RK, Rinaldo CR, Nowalk MP, Balasubramani GK, Moehling KK, Bullotta A, et al. Viral infections in outpatients with medically attended acute respiratory illness during the 2012–2013 influenza season. *BMC Infect Dis* 2015;15:87.

Zumla A, Al-Tawfiq JA, Enne VI, Kidd M, Drosten C, Breuer J, et al. Rapid point of care diagnostic tests for viral and bacterial respiratory tract infections—needs, advances, and future prospects. *Lancet Infect Dis* 2014:1123–35.